This article has been accepted for publication in IEEE/OSA Journal of Lightwave Technology. This is the author's version which has not been fully edited and content may change prior to final publication. Citation information: DOI 10.1109/JLT.2022.3225707

Reclaiming Light Dropped During Optical Modulation to Bias Avalanche Photodetectors

Bernhard Schrenk, *Member, IEEE,* and Margareta V. Stephanie, *Student Member, IEEE*

***Abstract*—The introduction of avalanche photodetectors in optical interconnects can extend the unallocated optical budget while unleashing further opportunities to migrate to novel datacenter network architectures. The required high-voltage rail that biases the photodiodes would involve a specialized electronic circuitry but will be instead harvested directly at the optical layer, taking advantage of the dropped power during optical modulation at local transmitters. Rather than dumping light resulting from extinct space bits, we will collect this contribution and convert it to a high-voltage bias by means of a photovoltaic power conversion circuit that is shared among and powered from all constituent data lanes of the optical interconnect. We will experimentally demonstrate that this energy reclamation circuit can sustain the sourced current during avalanche photodetection whilst maintaining a bias rail at ~25V with continuity, as will be proven for up to 64 data lanes. We demonstrate an optical budget of ~30 dB for 10 Gb/s/lane transmission, with a reception penalty as small as 0.2 dB with respect to an electrically biased photoreceiver. We will further elaborate on the limitations linked to the proposed concept, such as in terms of dynamic range.**

***Index Terms*—Optical communication terminals, Optical signal detection, Energy conversion, Optical interconnections**

I. Introduction

THE TREMENDOUS growth in information density concerning datacenters is driving the need for continuous upgrades in communication capacities. The interconnect bandwidth of switch cores has recently surpassed 10 Tb/s [1] and does not show any sign of saturation. Various solutions are being investigated at the optical layer in an attempt to support and sustain this growth in capacity, while maintaining an energy consumption in the fJ/bit range through electro-optic bandwidths of up to 100 GHz and ultra-small footprints [2]. Since further scaling of symbol rates becomes increasingly challenging, simplified coherent approaches are now being intensively researched for the very-short reach domain [3]. At the same time, inverse multiplexing is being explored for traditional direct-modulation / direct-detection systems in the context of massively-parallel interconnects. In this second approach, a "broad" Tb/s pipe is split into multiple "narrower" data lanes [4, 5]. In the extreme case, the number of data lanes can exceed 100 while the line rate is radically lowered, as recently demonstrated in an optical interconnect that featured low-complexity yet high energy-efficient optics such as micro-scale light emitting diodes operated at 2 Gb/s/lane in a 16×16 array configuration in combination with an imaging fiber bundle [6].

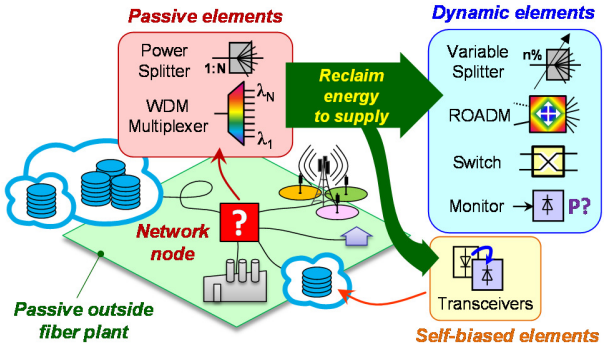

Fig. 1. Energy reclamation in optical networks and transceiver sub-systems.

However, the optical loss budget between transmitter and receiver of such interconnects is highly limited since high-speed opto-electronic signal converters at both ends should resort to conceptual simplicity. A possible migration path for increasing the optical budget under this constraint would be the use of avalanche photodetectors (APD) [7]. The provision of additional unallocated budget from doing so can enable novel network architectures that go beyond the simple point-to-point layout, as mostly found for optical interconnects. However, the generation of APD biases of typically >20V necessitates electronic integrated circuit processes with high breakdown voltage. Such are not supported by nanometer-scale CMOS technology nodes that particularly aim at a high degree of integration, high frequencies, and a lower nominal supply voltage. As the corresponding transistor voltage ratings scale down, the ability to synthesize high-voltage circuits is not given anymore. This makes the techno-economically attractive and performance-efficient monolithic integration of high-bandwidth electronics with high-voltage photonic elements, such as APDs, difficult.

In this work we leverage energy reclamation principles, as they have enjoyed the interest in optical communication networks with passive outside fiber plant (Fig. 1) where they are a resource to proliferate network functionality. Rather than

Manuscript received September 19, 2022. This work was supported in part by the European Research Council (ERC) under the European Union's Horizon 2020 research and innovation programme (grant agreement No 804769) and by the Austrian FFG agency through the JOLLYBEE project (grant No. 887467).

B. Schrenk and M. Stephanie are with the AIT Austrian Institute of Technology, Center for Digital Safety&Security, Giefinggasse 4, 1210 Vienna, Austria (phone: +43 50550-4131; fax: -4150; e-mail: bernhard.schrenk@ait.ac.at).

TABLE I
EXPERIMENTAL DEMONSTRATIONS OF OPTICAL-LAYER SUB-SYSTEMS SUPPLIED BY MEANS OF ENERGY SCAVENGING

Domain	Ref.	Scenario	Enabled function	Optically powered element	Accomplished performance	Energy harvesting characteristics
Optical signal distribution	[9]	Optical access	Reconfigurable power splitter	2×2 optical switches	Power allocation and multi-cast	Remote feed with 1480-nm pump (electr. power consumption of 1.5W)
	[10]	Optical access	Protection switching (resiliency)	2×2 optical switch, microprocessor	Fast response of ~10 ms incl. control plane response	Remote feed integrated with control plane channel (-10 dBm, 1480 nm)
	[11]	Metro-access PON	Reconfigurable optical add-drop	2×2 optical switches, microprocessor	Redistribution of optical spectrum in uni- and multi-cast	Remote feed integrated with control plane channel (-10 dBm, 1480 nm)
Integrated monitoring	[12]	Optical access	Power monitoring for splitter ports	Array of 8 photodiodes, microprocessor	Assignment of network units to splitter ports	Remote feed at -10 dBm optically
	[15]	WDM-overlaid PON	Optical spectrum monitoring	Spatial light modulator, photodetector, microprocessor	CWDM channel monitoring	Remote feed integrated with AMCC channel (-10 dBm, 1610 nm)
	[16]	Optical access	Optical time-domain reflectometry	2×2 optical switches, 1650 nm laser, photodetector, microprocessor	162ns OTDR pulses at 1650nm, acquisition at 20 MSa/s	Remote powering with 5 dBm at 1430 nm
Transceivers	[17]	Mobile fronthaul	Remote radio head for down- and uplink in sub-6GHz band	LNA, PA, PIN detector, VCSEL	Wireless 16-QAM OFDM reception over 84 dB of RF budget, incl. video streaming	Remote powering over standard single-mode fiber based fronthaul with optical pump of 290 mW
	[18]	Mobile fronthaul	Remote radio head for downlink in 94 GHz band	PIN detector, PA for 100 GHz	Wireless 16-QAM OFDM reception at 94 GHz over 1 meter	Remote powering at 1550 nm over multi-core fiber based fronthaul with 5×21 mW (aggregated over 5 cores)
	this work	Optical interconnects	APD instead of PIN receivers	64-lane APD bias (>20V) continuously supplied	Reception sensitivity of -24.1 dBm at 10 Gb/s, dynamic range of 3.6 dB	Re-use of power dropped during data modulation (6 dBm/lane)

remotely feeding flexible network nodes, we expand the concept of energy scavenging, for the first time to our best knowledge, to self-bias transceiver sub-systems in a manner where photonic instead of electronic circuits establish the required electrical supply rail at voltages beyond 25V. We do so by resorting to the fact that optical power is not "destroyed" during electro-optic data modulation but sunk to an unused photonic circuit branch, where it can be collected and reclaimed to generate an APD bias rail with a voltage beyond 20V. We experimentally prove the extension of the optical link budget for a bidirectional 1-, 2- and 4-lane short-reach optical interconnect through APD-enabled reception sensitivities of -24.1 dBm at 10 Gb/s/lane transmission, showing a negligible 0.2 dB penalty with respect to an electrical APD bias supply. These findings, which are based on our initial work in [8], are further extended by increasing the dimension of the optical interconnect to 64 lanes in order to investigate the sustainability of the energy reclamation concept toward a massive number of data lanes.

The paper is organized as follows. Section II introduces the adopted concept for the energy reclamation at the optical layer. Section III characterizes the capability of the photonic energy harvesting circuit to supply an APD bias. Section IV discusses the experimental arrangement used for performance evaluation. The corresponding results are then discussed in Section V. A comparison with conventional bias techniques is made in Section VI. Finally, Section VII concludes the work.

II. RECLAIMING ENERGY FROM DROPPED LIGHT TO SELF-BIAS LOCAL APD RECEIVERS

Reclaiming energy at the optical layer and converting light to a useful electrical supply that is tailored to the needs of the sub-system has been experimentally assessed during the past years. However, the efficiency of such concepts greatly depends on the actual application scenario and the sources that are available to scavenge from. Figure 2(a) highlights a few approaches towards this direction. The key notions behind these examples are as follows: *(i)* tap a small part of WDM signals and compensate the tapping loss of the signals through a slightly higher launch power for the involved and highly-efficient optical sources; *(ii)* reclaim power at unused splitter ports where optical power is available but not relayed any further; *(iii)* harvest and boost-convert power directly at the optical source, such as it is available at the back-facet of laser cavities; and *(iv)* modulation does not "destroy" optical power but sinks it to a "dead" end.

In all these cases, optical power that is already available will be reclaimed and eventually converted to an electrical supply through highly efficient opto-electronic circuits, its energy accumulated and stored, in order to be eventually depleted for later use. In the following we will highlight earlier state-of-the-art works, then introduce and relate the proposed concept of biasing APD detectors.

A. State-of-the-Art in Energy Harvesting at the Optical Layer

The adoption of energy scavenging methods at the optical layer has been mainly motivated by the rigidity of passive optical networks (PON) and primarily concerns access and metro networks (Fig. 1). Earlier works have identified the potential of reconfigurable network elements hosted in passive distribution networks, as summarized in Table I. Concerning the optical signal distribution, passive power splitters have been substituted by reconfigurable splitters with variable power ratio among their ports by including optical switches that are being fed remotely [9]. Similarly, optical switches that are remotely powered through a feed of -10 dBm have been incorporated deep inside the fiber plant to enhance resiliency, showing a fast response of 10 ms upon disconnecting the signal-relaying fiber of a dual-feeder trunk and the switch to the second trunk fiber, including control plane functionality

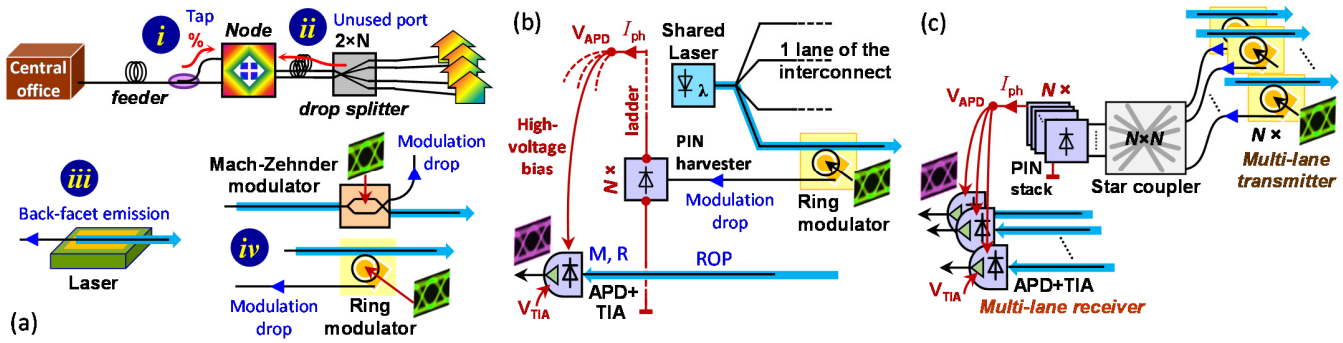

Fig. 2. (a) Energy reclamation opportunities and circuits with (b) dedicated photo-electric converter per modulation drop, or (c) shared energy converter.

[10]. Instead of switching the power ratio of splitters, spectral slices can be re-distributed among the ports of a remotely powered reconfigurable optical add-drop multiplexer (ROADM), as demonstrated in [11] with energy reclamation periods of 7 min between reconfigurations for a remote feed of -10 dBm. In most of these works, low-power microprocessors support signaling at an auxiliary control channel, while energy reclamation is based on photovoltaic power conversion with highly efficient electronic boost conversion and low-leakage capacitive energy reservoirs.

At the same time, monitoring functionality can be integrated with these remotely powered network nodes, supporting network operations, and allowing access to network segments that would otherwise be too remote to the operator's point of presence. Prior work has demonstrated the identification of network users connected to the ports of a splitter through binary power monitoring with an array of 8 photodiodes [12, 13] and intelligent demarcation points at the tail-end edge of an access network [14]. The spectral monitoring of a wavelength division multiplexed (WDM) feeder has been demonstrated using a remotely powered optical spectrum analyzer based on a liquid-crystal-on-silicon device serving as a spatial light modulator, allowing for an acquisition of the spectrum with coarse WDM (CWDM) resolution [15]. All these works on network monitoring have been conducted with a low optical feed level of -10 dBm. More recently, optical time-domain reflectometry (OTDR) has been demonstrated as remotely powered network monitoring function. The spans of all drop fibers connected to a 1×4 splitter have been analyzed through generation of 162-ns wide probe pulses at the splitter site and subsequent acquisition of the reflected optical echo through low-power analogue-to-digital conversion at 20 MSa/s. An accurate representation in terms of length and fiber transitions has been accomplished [16]. For this type of advanced functionality, the optical power feed had to be increased to 5 dBm in order to support the operation of higher-speed opto-electronics.

A further increase of optical feed power enables the remote supply of entire transceiver sub-systems at tail-end network units. This is especially interesting for network terminals that are not located at the customer premises but still remain at the outside fiber plant, such as antenna sites. Earlier works have investigated the possibility to supply remote radio heads (RRH) from a centralized office. Proof-of-concept works have experimentally demonstrated a bidirectional sub-6GHz macro-cell RRH [17] and a 94-GHz small-cell RRH [18]. A radio budget of 84 dB has been accomplished for the macro-cell case and confirmed through real-time video transmission. The required power feed is 290 mW for supplying multi-stage down- and uplink radio amplifier cascades [17]. Unidirectional 10-Gb/s downlink radio transmission over 1 m has been shown for the small-cell RRH, building on multi-core fiber to supply a feed of 5×21 mW to a 100-GHz photodetector with subsequent radio amplifier [18].

The concept presented in this work differs by not aiming at powering entire transceivers or network nodes at remote locations. The scope of the present experiment seeks to self-bias local transceiver subsystems such as an APD detector requiring a large bias voltage rather than being subject to a large electrical current consumption at a low-voltage supply.

B. Reclaiming a High-Voltage APD Bias

In order to scavenge an APD bias from unexploited optical power in an optical communication link, we propose to employ photoelectric conversion in a way that allows the aggregation of small contributions available at multiple communication lanes of a parallel optical interconnect. The proposed concept is introduced in Fig. 2. It relies on the collection of dropped light at the unused port of an interferometric modulator. The optical signal at this "dead" port is typically a complementary replica of the transmitted signal but often equals the transmitted signal in its optical power level, if a 50% ratio between mark and space bits applies.

As sketched in Fig. 2(b), this light can be explored as an additional energy source by collecting and harvesting it with an opto-electronic converter, which can be as simple as a PIN photodiode, ideally with a high responsivity and a low series resistance. By arranging these energy-converting photodiodes in a serialized photovoltaic ladder that spans over multiple data lanes, the generated voltage adds up and can lead to high values as required for APD biases, as we will prove shortly. The sourced current corresponds to the minimum current generated over all photodiodes involved in the ladder and is determined by the worst coupling between modulator drop port and PIN photodiode, including its responsivity.

The proposed scenario sketched in Fig. 2(b) stands in stark contrast to earlier works on optically driven energy harvesting

[9-18]. This is because prior works primarily focused on the provisioning of a large supply currents in the range of tens of mA required for a low-voltage actuation of opto-electro-mechanical elements such as latching switches. In this work, a large voltage of >20V needs to be generated, however, at a considerably lower sourced current. A second aspect is the continuity in supplied electrical power: While the pulsed actuation of elements such as latching optical switches features a highly asymmetrical duty cycle [9-11, 15, 16], the continuous data transfer necessitates the provisioning of an equally continuous APD bias. Therefore, no buffering or sequential boost conversion can be applied, and no trade-off can be made in terms of lowering the duty cycle.

An important aspect is the sustainability of the large APD bias voltage V_{apd} despite sourcing an increasing APD photocurrent at the same time. This photocurrent I_{ph} is generated by the received data signals and is determined by the received optical power (ROP) impinging onto multiple APDs that are supplied by the energy reclamation circuit. We shall consider N APDs that are characterized by a responsivity of R = 1 A/W. Operating these APDs at a multiplication factor of M = 10 would lead to a total photocurrent of

$$I_{ph} = N \cdot R \cdot M(V_{apd}) \cdot ROP \quad (1)$$

or $I_{ph} = N \cdot 32\mu A$ for a ROP of -25 dBm. It is important to note the dependence of M on the APD bias: The drain of a high photocurrent I_{ph} for a high ROP will place the energy harvester in a regime where it is unable to source the required current any longer. This will inevitably lead to a drop in the generated APD bias V_{apd} and, consequently, a reduced M, thus worsening the reception performance. As we will investigate through experimental studies, this will limit the dynamic range that can be accomplished when employing optically biased APD receivers as proposed and demonstrated in this work.

Since the experiment conducted in this work was not able to build on a plethora of N ring modulators, a slightly modified energy reclamation circuit (Fig. 2(c)) has been adopted. In this alternative arrangement, the elements of the PIN photodiode ladder are jointly fed by multiple modulator drop ports through a passive optical power distribution network. In detail, the drop ports of N data transmitters, operating at a generally random wavelengths, are shared among N PIN photodiodes by means of an $N \times N$ star coupler. This is roughly equivalent to the previous case since N dropped data signals now feed a single PIN photodiode, yet after passing the loss of an $N \times N$ split. With this, the proposed APD bias generator can accomplish and supply the same large APD bias voltage at a similar photocurrent but now from an arbitrary number of data lanes and, in particular, from a small number of lanes.

It shall be noted that the proposed energy reclamation circuit can be in principle implemented in a very compact way since neither star couplers nor photodiodes require a large footprint [19, 20].

III. Characterization of Energy Reclamation Circuit

The capability to generate a high-voltage APD bias through energy scavenging at the optical layer is quantified in Fig. 3. Characterization results are presented in terms of voltage-current (V-I) relations under load and are shown for various aggregated optical feed power levels. As a performance reference, we set an APD target voltage of 24.5V and investigate the photocurrent that can be sourced from the energy harvester.

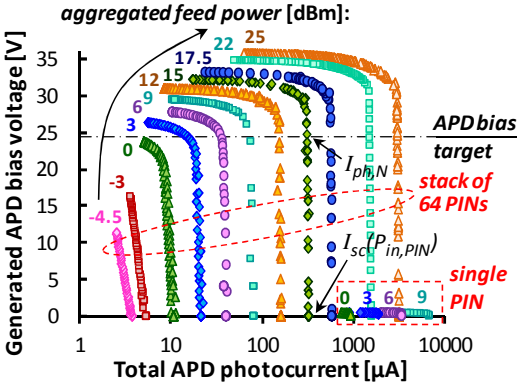

Fig. 3. V-I characteristics for the energy reclamation circuit for various optical feed power levels. Results are presented for a photo-electronic converter of the APD bias generator that is composed of a stack of 64 PIN photodiodes and, merely for comparison, by a single PIN photodiode.

The minimum aggregated power level to reach this target, which corresponds to the optical power that would have to be dropped by the modulators of all lanes, is 3 dBm in total. This is a relatively low value, considering that multiple lanes contribute to this feed and that the typically sourced power of lasers per lane is likely to be much higher in a realistic scenario. For example, in case of four constituent lanes, a modulation drop of -3 dBm would be sufficient to satisfy this condition. However, the permissible photocurrent at the receivers of all lanes is then only 15 µA. This rather low current $I_{ph,N}$ is closely related to the short-circuit current I_{sc} (Fig. 3), which is determined by the optical power $P_{in,PIN}$ arriving at a PIN element of the energy harvester after passing the splitting loss of the star coupler. Assuming again a scenario with four lanes and a ROP of -25 dBm for the reception of the data signals, the APD bias generator needs to already source a photocurrent of 126 µA for M = 10 and N = 4. To satisfy this condition, a total optical feed power of slightly less than 12 dBm is required, corresponding to a modulation drop of ~6 dBm per data lane.

Considering a larger number of 64 lanes, a considerably higher photocurrent of 2 mA needs to be sourced according to the aforementioned assumptions (ROP = -25 dBm, M = 10, N = 64). As Fig. 3 confirms, the V-I characteristics do not show a saturation effect towards a larger aggregated feed power: The APD bias generator can source a current of 1.5 and 3.1 mA for a total feed of 22 and 25 dBm, respectively. The latter features sufficient margin in terms of sourced current for the earlier mentioned case, while being slightly above the earlier 6 dBm/lane value for the modulation drop.

For the sake of comparison, Fig. 3 also presents the V-I characteristics of a single PIN photodiode acting as photoelectric energy converter. The generated voltage under

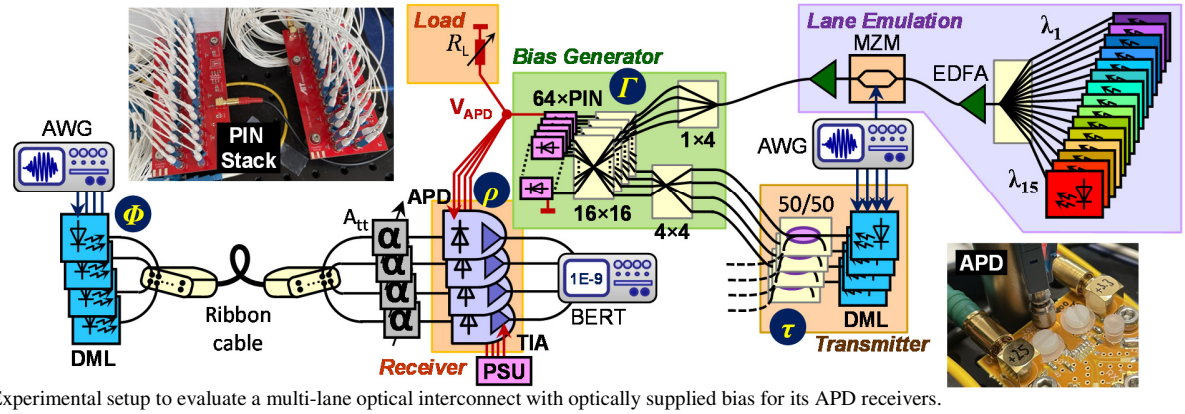

Fig. 4. Experimental setup to evaluate a multi-lane optical interconnect with optically supplied bias for its APD receivers.

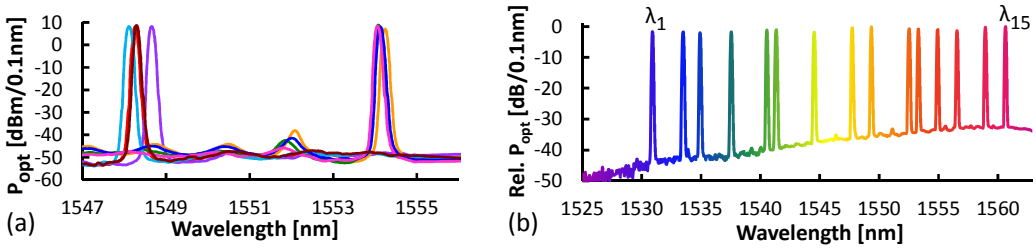

Fig. 5. Optical spectra for (a) the DMLs used as directly modulated optical emitters and (b) the DWDM comb that emulates the feed of further data lanes.

no-load conditions is 0.55V, while currents beyond 1 mA can be easily provisioned for feed power levels just slightly above 0 dBm. This is due to the absence of the passive 64-way split used to boost the output voltage and its low transmission between optical feed source and PIN photodiode.

The provision of the total APD photocurrent for all receivers at the data plane will further impact the dynamic range that is supported for data reception. This is because higher ROP levels lead to a rapidly increasing demand in photocurrent to be sourced by the energy reclamation circuit, eventually leading to an inevitable drop of M for APD-based data reception. For the specific case that the data lanes should adopt CWDM, the same multiplexing approach can be used for the signal distribution network feeding the PIN stack of the APD bias generator. This would greatly mitigate splitting loss, thus increasing the accomplishable power $P_{in,PIN}$ at the constituent PIN photodiodes of the photovoltaic energy converter and therefore the permissible photocurrent $I_{ph,N}$.

IV. Experimental Evaluation of a Multi-Lane Interconnect with Self-Biased APD Receivers

The experimental setup is presented in Fig. 4. It resembles a bidirectional interconnect with directly modulated lasers (DML) acting as 10 Gb/s optical emitters towards APD receivers. The DMLs feature an optical output power of 10 dBm and operate around 1550 nm, as shown in Fig. 5(a). Up to four data lanes have been implemented with DMLs, while further lanes have been emulated as described shortly.

At the transmitters (τ), the DMLs emulate the modulation and power-drop function of a ring modulator through appending an additional 50/50 coupler. In this way, each transmitter emits a modulated data signal with a launch power of 6 dBm towards the data plane while also feeding a modulated signal with the same power level to the APD bias generator (Γ) for the purpose of energy reclamation.

Energy scavenging builds on a 64×64 split configuration that employs 64 PIN diodes in photovoltaic mode. Due to the unavailability of an integrated star coupler with large port count, the 64×64 splitter has been composed by a 4×4 stage and four 16×16 stages. The dropped data signals of the transmitters feed the 4×4 stage, where the optical power is distributed to all 64 PIN photodiodes. The overall 64×64 splitter showed an average insertion loss of 19.7 dB. However, due to the serialized PIN photodiode stack, the maximum splitter loss determines the maximum current I_{sc} that can be sourced by the energy reclamation circuit. The loss distribution of the splitter is reported in Fig. 6 and the maximum port loss was 20.5 dB.

The 10-Gb/s data signals at the far end (Φ) of the bidirectional data plane are transmitted over a short MTP ribbon cable and delivered to the local receivers (ρ). We employed commercial APDs in ROSA package. These 10 Gb/s receivers were rated for a typical sensitivity of -25.5 dBm. The scavenged optical power of the local transmitters is converted to a high-voltage APD bias V_{apd}, which supplies all APD photodiodes of the receivers. As it is common when biasing photodiodes, a simple RC lowpass filter with a 100 Ω resistor and a 100 nF capacitor has been included to suppress noise artifacts in the bias line. As will be proven shortly by means of bit error ratio (BER) performance, this bias filter provides a sufficiently good suppression of residual data harmonics after optical bias generation. The corresponding transimpedance amplifiers (TIA) are instead supplied by an electrical power supply unit (PSU) delivering a low-voltage rail at 3.3V. Variable optical attenuators (A_{tt}) were used to set the ROP for real-time testing of the BER. This further allows

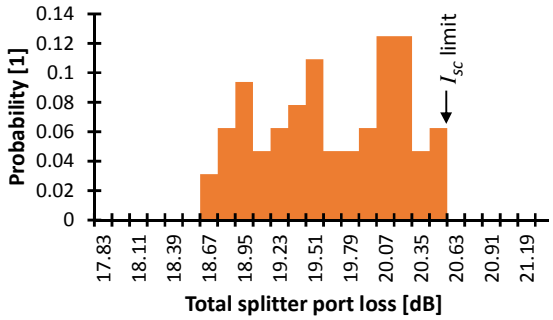

Fig. 6. Loss distribution for the 64×64 splitter.

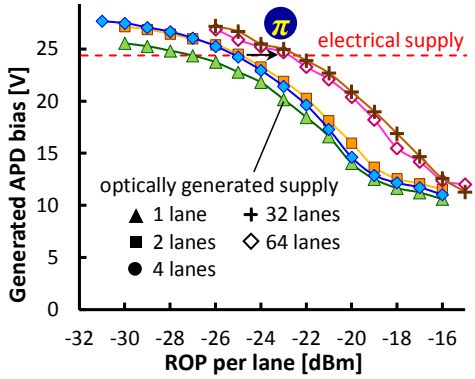

Fig. 7. APD bias voltage generated as function of the optical power received by the APD receiver at each data lane.

to investigate overload conditions for the bias generator that apply at higher ROP levels.

In order to allow an evaluation for more than four data lanes, the same large number of feed laser channels would be required to feed the data plane and the APD bias generator. Due to inventory issues, the missing optical sources have been extracted from an optical comb. To reach a high number of up to 60 additional sources feeding the bias generator, a comb of up to 15 dense WDM (DWDM) channels reaching from 1531.12 to 1560.61 nm (Fig. 5(b)) has been injected into every of the four 16×16 split stages that are constituent to the overall 64×64 split configuration. This is permissible since the passive star coupler preceding the PIN stack represents a wavelength-agnostic feed distribution network that operates independently of the transmitter wavelengths.

The DWDM comb has been modulated by a Mach-Zehnder modulator (MZM) with a 10 Gb/s signal, amplified by an Erbium-doped fiber amplifier (EDFA) and was adjusted with respect to its aggregated optical power in order to take the bypass of the first 4×4 split stage into account. In this way, the feed power is matched to that of the DML-based transmitters while a total feed of up to 64 channels is yielded for the purpose of energy scavenging. For a correct emulation of an intermediate number of lanes, a portion of the comb lines has been muted and the aggregated comb power has been adjusted accordingly.

On top of this, a larger number of lanes necessitates to emulate a larger number of APD receivers. For this purpose, a resistive load (R_L) has been used as a parallel current sink at the bias generator output. The load has been determined according to the photocurrent drawn by the actual APD detectors to account for the consumption of a fully occupied multi-lane receiver with up to 64 APDs. This process necessitates to iteratively adjust the load per ROP level since the generated APD bias V_{apd} is not constant but instead a function of the aggregated photocurrent drawn from the APD bias generator, owing to the characteristics of the photovoltaic energy harvester (Fig. 3).

V. Results and Discussion

The obtained APD bias for the multi-lane interconnect is reported in Fig. 7 for one (▲), two (■) and four lanes (●) with the earlier mentioned feed power of 6 dBm/lane at the modulation drop. The generated bias does not show a strong dependence on the number of lanes. This is because an increase in feed power due to additional transmitters is eroded by the extra current sink resulting from the same increase in APD receivers. Towards higher ROP levels, the APD bias falls below 15V for a ROP of about -20 dBm since the photocurrent for the APD receivers cannot be sustained any longer. In order to investigate the dependence of the APD bias on an increase in optical feed power, the corresponding feed for 32 (+) and 64 lanes (◇) has been increased by 1 dB to 7 dBm/lane. This 1-dB increase in feed power results in a shift (π) of the generated APD bias towards a higher sustainable ROP level as a larger photocurrent can not be sourced by the energy reclamation circuit. Specifically, it permits a 1.2 dB higher ROP at the reference bias level of 24.5 V.

The BER performance for several link configurations is presented in Fig. 8. As a reference, we have included the reception performance for an electrically supplied APD receiver, which showed a sensitivity of -24.3 dBm (×) at a BER of 10^{-10}.

For a 4-lane interconnect with optically supplied APD bias (◆) at a feed of 6 dBm/lane, the penalty in reception sensitivity was 0.2 dB in average. This proves the correct operation of the energy reclamation circuit and the sufficiently high suppression of residual data harmonics through the RC bias filter. It further evidences that the optical budget can be significantly boosted to ~30 dB at 10 Gb/s, by virtue of the APD gain. The aforementioned drop of the APD bias with increasing ROP (Fig. 7) manifests itself in a limited dynamic range: The BER of 10^{-10} is surpassed for a ROP of -20.3 dBm or higher, resulting in a dynamic range of 4.2 dB in average. However, compared to the current situation in high-bandwidth intra-datacenter links that are subject to high-baudrate signalling, similar dynamic range limitations apply due to a greatly limited optical budget in the range of 6 dB [21].

The BER performance for a smaller number of two (■) and one (●) data lanes shows similar reception sensitivities of -23.7 and -23.3 dBm, respectively. The penalty with respect to the reference receiver thus remained within a 1-dB range. Moreover, a similar dynamic range as for the 4-lane interconnect has been found, as summarized in Fig. 9 for the two reference BER levels of 10^{-10} and 10^{-3}.

Finally, we have acquired the BER performance for

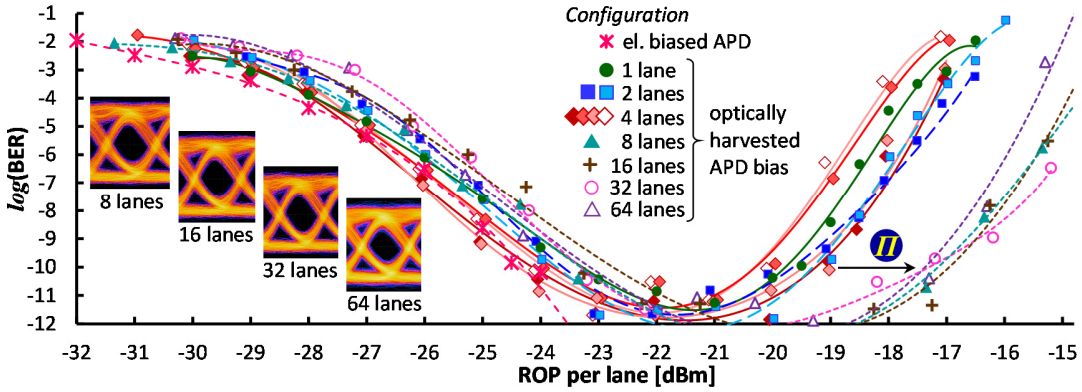

Fig. 8. BER performance for various configurations of the optical interconnect, reaching from 1 to 64 data lanes.

interconnects that emulate a larger number of 8 (▲), 16 (+), 32 (○) and 64 (△) data lanes. Again, we have maintained the 1-dB increase in feed power as in Fig. 7 in order to evaluate the dependence of the BER on different feed power levels. While the reception sensitivity at lower ROP values is not impacted significantly and remains within a range of 1.1 dB, the BER increase in the overload regime at higher ROP is shifted by up to 2.7 dB towards larger ROP values (*II*). Consequently, the dynamic range increases by 1.6 dB in average at a BER of 10^{-10}. This is expected since a higher APD bias can be maintained, as earlier discussed in Fig. 7. The eye diagrams that are included as inset in Fig. 8 have been acquired at a ROP of -22 dBm.

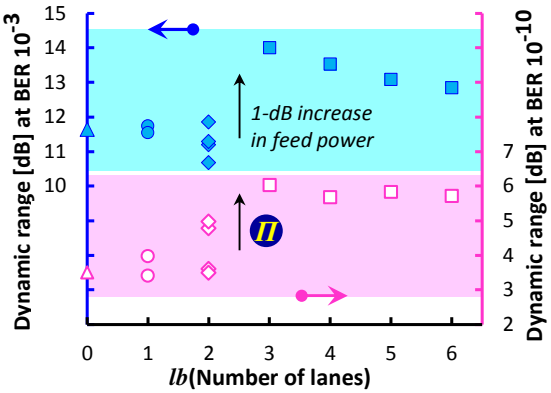

Fig. 9. Supported dynamic range as function of the number of data lanes.

VI. Comparison with Conventional Techniques

The provision of an optical bias generator circuit features several advantages compared to a conventional approach with an externally provisioned APD bias.

First, the respective optical circuit can be fitted on the optical layer of a transceiver arrangement, by virtue of its compact size. Considering the receiving sub-system of a 64-lane transceiver, an area of 0.013 and 32 mm² have to be accounted for the APD photodiodes and their TIAs, respectively [2]. The bias generator itself requires a ladder of 64 PIN photodiodes with a footprint of 0.002 mm² and a star coupler. The latter can be realized on a footprint of less than 10 mm² [20], with large potential for an even more compact structure [22]. This means that the APD bias generator can be included at the optical layer without increasing the footprint of the opto-electronic transceiver, which is instead limited by the size of the multi-channel TIA. On the contrary, providing an APD bias with an external bias circuit such as a boost converter or a charge pump would require *(i)* an extra chip die for the converter and *(ii)* extra capacitive or inductive components with element values that cannot be realized on-chip. Therefore, a compact footprint as provided through the proposed optical bias circuit cannot be maintained.

Moreover, the multi-chip arrangement of a conventional external bias supply requires extra die-attach tasks and extra supply ports for the multi-lane transceiver. Both raises the assembly cost, which is known to be a dominant portion in the cost structure of optical transceivers [23]. By co-integrating an optical bias circuit as demonstrated in this work, this cost contribution can be effectively mitigated.

VII. Conclusion

We have explored the principle of energy reclamation at the optical layer to generate an electrical APD supply in order to boost the unallocated budget of optical interconnects. We have experimentally proven that an APD bias in the order of 25V can be established through a photovoltaic power conversion circuit that is shared by up to 64 data lanes whose dropped optical power during modulation of space bits at the corresponding transmitters serves as energy source for the APD bias generator. We showed that the accomplished APD biasing comes with a negligible reception penalty of 0.2 dB with respect to an electrically biased APD receiver. Moreover, the sensitivity, which was -24.1 dBm at BER of 10^{-10} for 10 Gb/s/lane transmission over 4 lanes, is widely independent on the number of data lanes, for which up to 64 transmitter-receiver pairs have been emulated experimentally. The current limitation in dynamic range (4.2 dB for 4 lanes) requires a re-design of the energy reclamation circuit to support a higher photocurrent sourced by the APD receivers for higher ROP levels. The extension of the optical budget to ~30 dB permits an exploration on novel architectures for intra-datacenter networks.

REFERENCES

[1] A. Agrawal, and C. Kim, "Intel Tofino2 – A 12.9Tbps P4-Programmable Ethernet Switch," in *Proc. 2020 IEEE Hot Chips 32 Symposium (HCS)*, 2020.

[2] C. Thraskias *et al.*, "Survey of Photonic and Plasmonic Interconnect Technologies for Intra-Datacenter and High-Performance Computing Communications," *IEEE Comm. Surveys & Tutorials*, vol. 20, no. 4, pp. 2758-2783, Fourthquarter 2018.

[3] B. Buscaino, B. D. Taylor, and J. M. Kahn, "Multi-Tb/s-per-Fiber Coherent Co-packaged Optical Interfaces for Data Center Switches," *J. of Lightwave Technol.*, vol. 37, no. 13, pp. 3401-3412, Jul. 2019.

[4] D. Butler *et al.*, "Space Division Multiplexing in Short Reach Optical Interconnects," *J. Lightwave Technol.*, vol. 35, pp. 677-682, 2016.

[5] D. Piehler, "Optical interconnects in enterprise and hyperscale datacenters," in *Proc. SPIE 11286, Opt. Int. XX*, p. 1128602, 2020.

[6] B. Pezeshki, F. Khoeini, A. Tselikov, R. Kalman, C. Danesh, and E. Afifi, "MicroLED Array-based Optical Links Using Imaging Fiber for Chip-to-chip Communications," in *Proc. Opt. Fiber Comm. Conf. (OFC)*, San Diego, United States, Mar. 2022, paper W1E.1.

[7] Q. Cheng, M. Bahadori, M. Glick, S. Rumley, and K. Bergman, "Recent advances in optical technologies for data centers: a review," *Optica*, vol. 5, no. 11, pp. 1354-1370, Nov. 2018.

[8] B. Schrenk, and M.V. Stephanie, "Reclaiming High-Voltage APD Biases From Dropped Optical Data Signals of Multi-Lane Interconnects," in *Proc. Europ. Conf. Opt. Comm. (ECOC)*, Basel, Switzerland, Sep. 2022, paper We5.46.

[9] Y. Bi, J. Jin, A.R. Dhaini, and L.G. Kazovsky, "QPAR: A Quasi-Passive Reconfigurable Green Node for Dynamic Resource Management in Optical Access Networks," *J. Lightwave Technol.*, vol. 32, no. 6, pp. 1104-1115, 2014.

[10] B. Schrenk, A. Poppe, M. Stierle, and H. Leopold, "Fully-Passive Optical Switch Introducing Dynamicity and Flexibility to Metro-Access", *IEEE Phot. Technol. Lett.*, vol. 27, pp. 486-489, Mar. 2015.

[11] B. Schrenk *et al.*, "Passive ROADM Flexibility in Optical Access with Spectral and Spatial Reconfigurability," *IEEE J. Sel. Areas in Comm.*, vol. 33, no. 12, pp. 2837-2846, 2015.

[12] J. Hehman, M. Straub, L. Jentsch, M. Earnshaw, P. Anthapadmanabhan, and T. Pfeiffer, "Remotely Powered Intelligent Splitter Monitor for Fiber Access Networks," in *Proc. Europ. Conf. Opt. Comm. (ECOC)*, Valencia, Spain, Sep. 2015, paper Tu.1.5.4.

[13] P. Iannone *et al.*, "An 8- × 10-Gb/s 42-km High-Split TWDM PON Featuring Distributed Raman Amplification and a Remotely Powered Intelligent Splitter," *J. Lightwave Technol.*, vol. 35, no. 7, pp. 1328-1332, 2017.

[14] M. Straub, V. Hückstädt, M. Ulrich, T. Pfeiffer, and R. Bonk, "Field Trial of a System-Independent Infrastructure Monitoring System for Access Networks," in *Proc. Opt. Fiber Comm. Conf. (OFC),* San Francisco, United States, Mar. 2021, paper M3F.3.

[15] B. Schrenk, M. Hofer, M. Hentschel, and T. Zemen, "Energy Self-Sufficient Node With Integrated Lightpath Monitoring for Spectrum-Aware PON," *IEEE Phot. Technol. Lett.*, vol. 29, pp. 318-321, Feb. 2017.

[16] M. Straub, L. Jentsch, J. Hehmann, T. Pfeiffer, and R. Bonk, "Remotely Powered Inline OTDR Unit with Unique Identification Possibility of Power Splitter Branches for Use in Access Network Applications," in *Proc. Europ. Conf. Opt. Comm. (ECOC)*, Rome, Italy, Sep. 2018, paper We2.68.

[17] B. Schrenk, and T. Zemen, "Real-Time Demonstration of an Optically Powered Radio Head for Low-Power Small Cells with 94 dB End-to-End Budget," in *Proc. Europ. Conf. Opt. Comm. (ECOC)*, Dusseldorf, Germany, Sept. 2016, paper Th.2.P2.SC7.10.

[18] T. Umezawa *et al.*, "Multi-Core Based 94-GHz Radio and Power over Fiber Transmission Using 100-GHz Analog Photoreceiver," in *Proc. Europ. Conf. Opt. Comm. (ECOC)*, Dusseldorf, Germany, Sep. 2016, paper Th.2.P2.SC7.2.

[19] P.D. Trinh, S. Yegnanarayanan, and B. Jalali, "5x9 Integrated Optical Star Coupler in Silicon-on-Insulator Technology," *IEEE Phot. Technol. Lett.*, vol. 8, no. 6, pp. 794-796, Jun. 1996.

[20] G.B. Cao, L.J. Dai, Y.J. Wang, J. Jiang, H. Yang, and F. Zhang, "Compact Integrated Star Coupler on Silicon-on-Insulator," *IEEE Phot. Technol. Lett.*, vol. 17, no. 12, pp. 2616-2618, Dec. 2005.

[21] X. Zhou, R. Urata, and H. Liu, "Beyond 1 Tb/s Intra-Data Center Interconnect Technology: IM-DD OR Coherent?," *J. Lightwave Technol.*, vol. 38, no. 2, pp. 475-484, 2020.

[22] R. Huang *et al.*, "Design of an Ultra-compact Star-coupler Based 1×10 Power Splitter with Nano-pixel Structures," in *Proc. IEEE 17th Int. Conf. on Group IV Photonics (GFP)*, Malaga, Spain, Dec. 2021, paper ThB2.2.

[23] T. Barwicz *et al.*, "Automated, high-throughput photonic packaging," *Optical Fiber Technology*, vol. 44, pp. 24-35, Aug. 2018.